

The Collatz tree as a Hilbert hotel: an automorphism proof of the $3x + 1$ conjecture

Jan Kleinnijenhuis¹, Alissa M. Kleinnijenhuis^{2, 3}, and Mustafa G. Aydogan⁴

¹Vrije Universiteit Amsterdam, The Network Institute
j.kleinnijenhuis@vu.nl

²University of Oxford, INET, Mathematical Institute
alissa.kleinnijenhuis@maths.ox.ac.uk

³Stanford University, Institute for Economic Policy Research
amklein@stanford.edu

⁴University of California San Francisco, Department of Biochemistry and Biophysics
mustafa.aydogan@ucsf.edu

December 13, 2021

Abstract

To be proven is that the *Collatz function*, which repeatedly converses even numbers n to $n/2$, and odd ones to $3n+1$, gives all numbers a root path to 1 in the Collatz tree. We picture its binary subtree of branching nodes with an upward child in the $2n$ direction and a rightward child in the $(n-1)/3$ direction. Consecutive generations of upward successors of rightward numbers, and of rightward successors of upward numbers, can be moved into two series of disjoint subtrees through two unary functions that define a tree automorphism group. Dispersed successors, identifiable by their congruence class, inherit a second root path via their subtree. The cumulative density of subtree congruence classes amounts to 1. Therefore, all numbers have a root path to 1.

The Collatz conjuncture holds that the Collatz function $C(n) = n/2$ if n is even, but $C(n) = 3n+1$ if n is odd, reaches 1 for all natural numbers n , in a finite *root path* of iterations that result in a unique sequence of numbers that either expand or contract (see a few examples below).

$8 \rightarrow 4 \rightarrow 2 \rightarrow 1$ ($\rightarrow 4 \rightarrow 2 \rightarrow 1 \rightarrow \dots$)

$9 \rightarrow 28 \rightarrow 14 \rightarrow 7 \rightarrow 22 \rightarrow 11 \rightarrow 34 \rightarrow 17 \rightarrow 52 \rightarrow 26 \rightarrow 13 \rightarrow 40 \rightarrow 20 \rightarrow 10 \rightarrow 5 \rightarrow 16 \rightarrow 8 \rightarrow 4 \rightarrow 2 \rightarrow 1$

$10 \rightarrow 5 \rightarrow 16 \rightarrow 8 \rightarrow 4 \rightarrow 2 \rightarrow 1$

This one-sentence, relatively simple-looking conjecture has become world renowned after numerous attempts by both famous, and amateur, mathematicians demonstrated that its proof is anything but straightforward. The problem appeared to be “representative of a large class of problems concerning the behavior under iteration of maps that are expanding on part of their domain and contracting on another part of their domain” [1]. In the words of Paul Erdős (1913–1996): “hopeless, absolutely hopeless” [1]. Numerical computations verified the conjecture for all numbers below 2^{68} [2]. In his recent paper that postulates a proof for “almost all” numbers, Terence Tao states that “a full resolution of the conjecture remains well beyond current methods” [3].

Jeffrey Lagarias, the editor of a seminal book on the conjecture, sets out how the conjecture “cuts across” many different fields of mathematics [1]. One hitherto insufficient approach to prove the Collatz conjecture, outlined by Marc Chamberland, is to find *ever less dense* node subsets $S \subset \mathbb{N}$, such that a proof on S implies that it is true on \mathbb{N} [5]. The natural density of a subset S is the proportion of numbers in S within a range, or *period*, of successive numbers (e.g. one out of two numbers in any period of 2 is odd). Tao’s recent logarithmic density proof for “almost all numbers” is based on the set S of *odd* numbers in a remaining “Syracuse tree”, which excludes also the even branching nodes (Fig. 1, green or red numbers) [3]. As noted by Tao [3] and also by Kontorovich [6, 7], this result still allows for exceptions, and even for the possibility that the conjecture is undecidable.

We follow Lothar Collatz (1910–1990), who specifically hoped to establish new “connections between elementary number theory and elementary graph theory”, “using the fact that one can picture a number theoretic function $f(n)$ with a directed graph” where each iteration is with “an arrow from n to $f(n)$ ” [8]. We picture a binary subtree with as its nodes the branching numbers in the Collatz tree and as its arrows the paths connecting them (Fig. 1, green or red). We define two functions for which the alternations and iterations generate the root paths to numbers from two infinite series of disjoint subtrees with cyclic roots on the trivial trunk or the greedy branch. The disjoint node sets $S \subset \mathbb{N}$ of the two series of subtrees can be detailed further as congruence classes, the cumulative density of which covers all natural numbers, thereby proving that $N_C = \mathbb{N}$. Isolated trajectories do not exist.

2 Disclosing binary tree $T_{\geq 0}$

In Figure 1 of the Collatz tree, the green and red colors of arrows in the paths to green and red branching numbers already highlight its infinite binary subtree $T_{\geq 0}$ shown in Figure 2. The uncolored numbers in Figure 1 do not branch further in two directions.

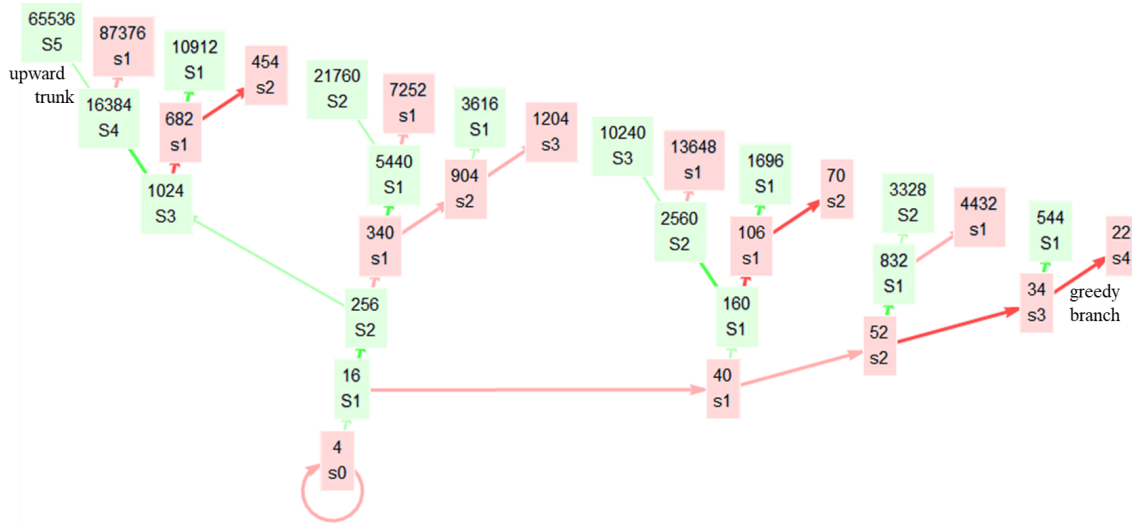


Figure 2: Binary tree $T_{\geq 0}$ with cyclic root $\Omega_{\geq 0} = 4$

Numbers connected by $(n-1)/3$ to numbers divisible by 3 are uncolored because their $2n$ successors cannot branch in the $(n-1)/3$ direction (Fig. 1, dashed orbits). The uncolored numbers reduce through iterations of the Collatz function to green or red numbers on branching nodes, labeled as set $S_{\geq 0}$.

Each number's upward, green-colored, child is defined by the upward function $U_0 : S_{\geq 0} \rightarrow S_{\geq 1}$; $U_0(n) = \text{Argmin}_p n \cdot 2^p$, in which Argmin_p is the argument minimization function that minimizes the number p of $2n$ steps to reach a child in the $2n$ direction. For example, the expanding upward path $16 \rightarrow 32 \rightarrow 64 \rightarrow 128 \rightarrow 256$ (Fig. 1) gives $p = 4$. A first contracting $(n-1)/3$ step is required to reach the rightward child, with a number p of $2n$ steps thereafter. This process defines the rightward function $R_0 : S_{\geq 0} \rightarrow S_0$; $R_0(n) = \text{Argmin}_p (n-1)/3 \cdot 2^p$. For example, the path $16 \rightarrow 5 \rightarrow 10 \rightarrow 20 \rightarrow 40$ (Fig. 1) gives $p = 3$.

3 Defining subtrees of automorphic tree $T_{\geq 0}$

The standard definition of $T_{\geq 0}$ as a graph $G = (V, E)$ with a set of nodes, or $V(\text{ertices}) S_{\geq 1}$, and S_0 , and a set of arrows or $E(\text{dges}) S_{\geq 0} \rightarrow S_{\geq 1}$ and $S_{\geq 0} \rightarrow S_0$ (definition 1) is not particularly helpful to arrive at the node sets $S \subset \mathbb{N}$ of its subtrees.

Definition 1. $T_{\geq 0} = (S_{\geq 0}, S_{\geq 0} \rightarrow S_{\geq 1}, S_{\geq 0} \rightarrow S_0)$

Following Collatz, we include the upward and rightward functions U_0 and R_0 that define its two arrows subsets, which render through a binary split its two node subsets (definition 2).

Definition 2. $T_{\geq 0} = \left(\begin{array}{l} U_0 : S_{\geq 0} \rightarrow S_{\geq 1} \text{ (Fig.2, upward arrows, green)} \\ R_0 : S_{\geq 0} \rightarrow S_0 \text{ (Fig.2, rightward arrows, red)} \end{array} \right)$

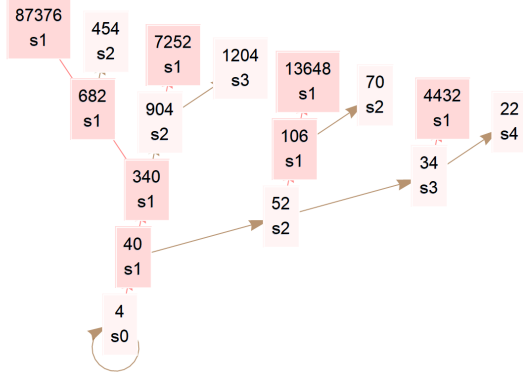
Their iterations U_0^j and R_0^k , with iterations denoted by superscripts j and k , define immediately the rightward and upward paths of arrows that alternately appear in root paths (definition 3). Each upward number (Fig. 2, green nodes) is the *unary* ancestor, or argument, of rightward successors s_1, s_2, s_3, \dots (Fig. 2, red orbits). For example, $R_0^3(256 \in S_{\geq 1}) = (1204 \in s_3)$ is the ancestor of the rightward path $256 \rightarrow 340 \rightarrow 904 \rightarrow 1204 \rightarrow \dots$. Reversely, each rightward number (Fig. 2, red nodes) is the unary ancestor of upward successors S_1, S_2, S_3, \dots (Fig. 2, green orbits). For example, $U_0^3(40 \in s_1 \subset S_0) = (10240 \in S_3)$ is the ancestor of the upward path $40 \rightarrow 160 \rightarrow 2560 \rightarrow 10240 \rightarrow \dots$. Rightward iterations also generate the cyclic root $\Omega_{\geq 0} = R_0^k(4) = 4$ with successor level s_0 .

Definition 3. $T_{\geq 0} = \left(\begin{array}{l} U_0^j : S_0 \rightarrow S_j, \text{ for } j = 1, 2, 3, \dots \text{ (Fig.2, upward paths, green)} \\ R_0^k : \Omega_{\geq 0} \rightarrow \Omega_{\geq 0}, S_{\geq 1} \rightarrow s_k \text{ for } k = 1, 2, 3, \dots \text{ (rightward paths, red)} \end{array} \right)$

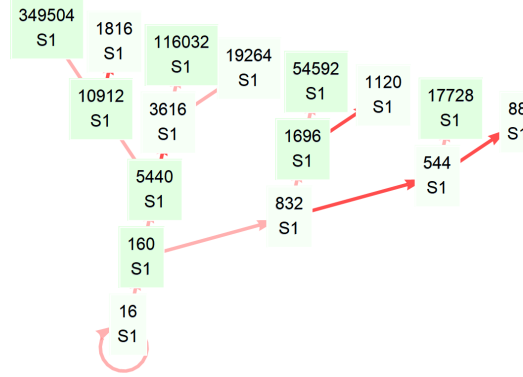
Following definition 3, our choice of subsets $S \subset \mathbb{N}$ to prove the Collatz conjecture consists of generations of upward and rightward successors S_1, S_2, S_3, \dots , respectively s_1, s_2, s_3, \dots . Figure 2 shows that each generation of upward or rightward successors is scattered across the entire tree $T_{\geq 0}$. We determine the moves to gather each upward generation S_1, S_2, S_3, \dots , respectively rightward generation s_1, s_2, s_3, \dots in its entirety in a correspondingly labeled upward subtree T_1, T_2, T_3, \dots (Fig. 3) or rightward subtree t_1, t_2, t_3, \dots (Fig. 4). Our tailored definition (definition 4) and the equivalent commutative diagram (Fig. 5) of the *automorphism group* of the binary tree $\text{Aut}(T_{\geq 0}, U_0, R_0)$ capture the fact that these moves give in successive generational subtrees *corresponding nodes* to

each other's ancestors and successors while giving within each generational subtree *conjugate arrows* that are interconnected to *second root paths* in tree $T_{\geq 0}$. *Automorphism* entails that moving the root of any *isomorphic* subtree towards the root of the tree reveals the one-to-one correspondence between their nodes and arrows [9, 10, 11] (Figs. 3–4).

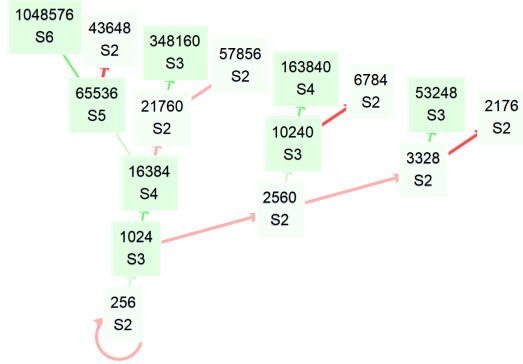
In $T_{\geq 0}$ (Fig. 2), move 1 node leftwards
 $T_0 = R_0(T_{\geq 0})$, trivial root $\omega_{\geq 0} = \Omega_{\geq 0} = 4$,
 inner arrows $T_0(U_1, R_0)$



In $T_{\geq 0}$, 1 node leftwards, next 1 node downwards
 $T_1 = U_0^1 R_0(T_{\geq 0})$, trivial trunk root $\Omega_1 = 16$,
 inner arrows $T_1(U_0^1 U_1 U_0^1, R_1)$



In $T_{\geq 0}$, 1 node leftwards, next 2 nodes downwards
 $T_2 = U_0^2 R_0(T_{\geq 0})$, trivial trunk root $\Omega_2 = 256$,
 inner arrows $T_2(U_0^2 U_1 U_0^2, R_2)$



In $T_{\geq 0}$, 1 node leftwards, next 3 nodes downwards
 $T_3 = U_0^3 R_0(T_{\geq 0})$, trivial trunk root $\Omega_3 = 1024$,
 inner arrows $T_3(U_0^3 U_1 U_0^3, R_3)$

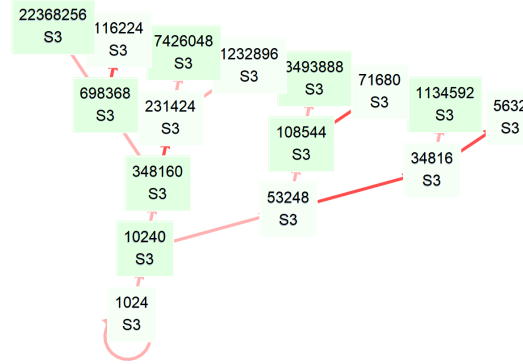


Figure 3: Rightward subtree T_0 and its upward successor subtrees T_1, T_2, T_3, \dots

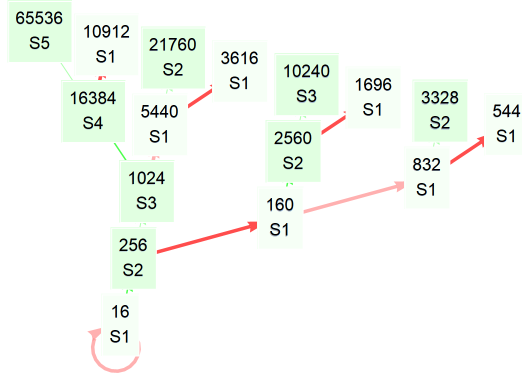
3.1 Successors receive corresponding nodes

A leftwards move of the numbers in tree $T_{\geq 0}$ generates a rightward tree T_0 with rightward orbits $s_1 \rightarrow s_2 \rightarrow s_3 \rightarrow \dots$ without their upward argument $S_{\geq 1} \rightarrow \dots$ (Fig. 3, top left). The rightward orbit $340 \rightarrow 904 \rightarrow 1204 \rightarrow \dots$ pushes out its argument $256 \rightarrow \dots$. Because rightward children take the nodes in tree T_0 , this *leftward move* is defined by the *rightward function*, written as $T_0 = R_0(T_{\geq 0}) =$

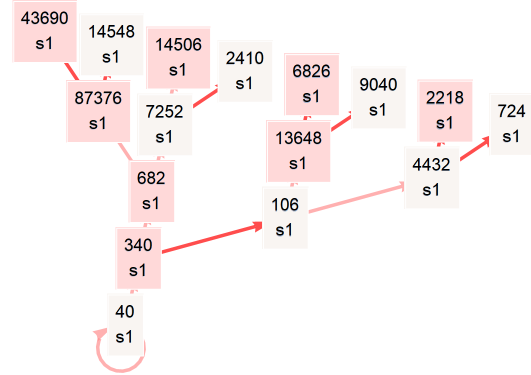
$R_0 T_{\geq 0}$. Conversely, a downward move (Fig. 4, top left) generates the upward tree $T_{\geq 1} = U_0(T_{\geq 0})$ with upward orbits $S_1 \rightarrow S_2 \rightarrow S_3 \rightarrow \dots$ without a rightward ancestor $s_{\geq 1} \rightarrow \dots$. The upward orbit $160 \rightarrow 2560 \rightarrow 10240 \rightarrow \dots$ ousts its rightward argument $40 \rightarrow \dots$.

Downward moves of upward successor subsets S_1, S_2, S_3, \dots bring them to the nodes of the rightward numbers in tree T_0 , which were the nodes of upward numbers in tree $T_{\geq 0}$. Thus, the node of the rightward argument 40 is taken by its upward successors $160 \rightarrow 2560 \rightarrow 10240 \rightarrow \dots$ (Fig. 2) in successive upward subtrees T_1, T_2 , and T_3 (Fig. 3). This process shows why each upward subtree is defined as $T_j = U^j(T_0) = U^j R_0(T_{\geq 0})$. Conversely, any rightward subtree is defined as $t_k = R^k U_0(T_{\geq 0})$. For example, see that the node of the upward argument 256 is taken by its rightward successors $340 \rightarrow 904 \rightarrow 1204 \rightarrow \dots$ (Fig. 2) in successive rightward subtrees t_1, t_2 , and t_3 (Fig. 4).

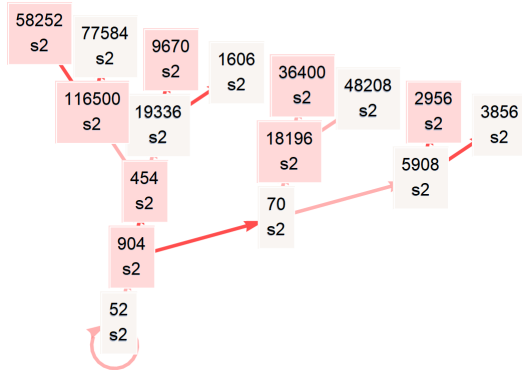
In $T_{\geq 0}$ (Fig. 2), move 1 node downwards:
 $T_{\geq 1} = U_0(T_{\geq 0})$, upward trunk root $\Omega_{\geq 1} = 16$,
 inner arrows $T_{\geq 1}(U_0, R_1)$



In $T_{\geq 0}$, 1 downwards, next 1 node leftwards:
 $t_1 = R_0^1 U_0(T_{\geq 0})$, greedy branch root $\omega_1 = 40$,
 inner arrows $t_1(U_1, R_{1,1} = R_0^1 R_1 R_0^{-1})$



In $T_{\geq 0}$, 1 node downwards, next 2 nodes leftwards:
 $t_2 = R_0^2 U_0(T_{\geq 0})$, greedy branch root $\omega_2 = 52$,
 inner arrows $t_2(U_2, R_{2,1} = R_0^2 R_1 R_0^{-2})$



In $T_{\geq 0}$, 1 node downwards, next 3 nodes leftwards:
 $t_3 = R_0^3 U_0(T_{\geq 0})$, greedy branch root $\omega_3 = 34$,
 inner arrows $t_3(U_3, R_{3,1} = R_0^3 R_1 R_0^{-3})$

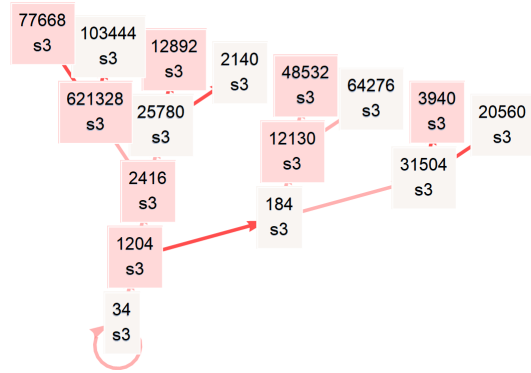


Figure 4: Upward subtree $T_{\geq 1}$ and its rightward successor subtrees t_1, t_2, t_3, \dots

The Collatz tree resembles an infinite fully booked Hilbert hotel, named after its inventor David

Hilbert (1862–1943), which accepts infinitely many new guests because its present guests can move to higher numbered rooms [12]. The departure of either the upward or the rightward infinite subset leaves the hotel fully booked (Figs.3–4, top left), after which the two departed sets split in two infinite series of subsets, each of which can re-occupy all of its rooms (Figs.3–4).

3.2 Paired successors receive conjugated arrows

Moving numbers become connected to fellow travelers as they reach connected nodes. The *conjugated* pair-of-pairs function $f_i = g^i f_0 g^{-i}$ applies, also referred to as the inner automorphism function, or, after its pioneer Max Dehn (1878–1952), the transformation function [13]. See, for example, the paired rightward successors $16 \rightarrow 40 \rightarrow 52 \rightarrow 34 \rightarrow \dots$ and $256 \rightarrow 340 \rightarrow 904 \rightarrow 1204 \rightarrow \dots$ of connected upward ancestors $16 \rightarrow 256$ (Fig. 2). In the rightward subtrees t_1, t_2 , and t_3 (Fig. 4), they give successively the conjugated upward connections $U_1(40) = 340$, $U_2(52) = 904$, and $U_3(34) = 1204$ (Fig. 4), with as their general specification $U_j = R_0^j U_0 R_0^{-j}$, with subscripts to denote conjugations. Conversely, in an upward subtree T_j , paired upward numbers become conjugate rightward connections $R_k = U_0^k R_0 U_0^{-k}$. For example, see how $R_2(2560) = 3328$ in tree T_2 (Fig. 3, bottom left) reflects $R_0(40) = 52$ in tree $T_{\geq 0}$ (Fig. 2).

Upward arrows in upward subtrees rest on two nested conjugations denoted as $U_{j,1} = U^j U_1 U^{-j} = U^j R_0^1 U_0 R_0^{-1} U^{-j}$. See, for example, in tree $T_{\geq 0}$ the orbits $16 \rightarrow 40 \rightarrow 160 \rightarrow 2560 \rightarrow \dots$ and $256 \rightarrow 340 \rightarrow 5440 \rightarrow 21760 \rightarrow \dots$ that are paired by $U_0 : 16 \rightarrow 256$. In tree T_2 , we obtain, therefore, $U_{2,1} = U^2 U_1 U^{-2} : 2560 \rightarrow 21760$ (Fig. 2). Conversely, rightward arrows in rightward subtrees become $R_{k,1} = R^k R_1 R^{-k} = R^k U_0^1 R_0 U_0^{-1} R^{-k}$. For example, see how $R_{2,1}(904) = 70$ in tree t_2 (Fig. 4, bottom left) reflects $R_0(16) = 40$ in tree $T_{\geq 0}$ (Fig. 2).

3.3 Successors receive a second subtree root path

Our tailored definition of the automorphism group $\text{Aut}(T_{\geq 0}, U_0, R_0)$ of tree $T_{\geq 0}$ (definition 4) summarizes the findings above on corresponding nodes and conjugated arrows in subtrees labeled with the depth-first schemes T_1, T_2, T_3, \dots and t_1, t_2, t_3, \dots . Existing definitions [9, 14] assume breadth-first labeling, which becomes intractable if iterations of the two underlying *unary* functions behave as differently as those of U_0 (expansions only) and R_0 (also contractions). The key to definition 4 is the distinction between upward and rightward subtrees (T or t), and next between nested or disjoint subtrees ($T_{\geq j}$ or T_j , $t_{\geq k}$ or t_k).

Definition 4. The automorphism group $\text{Aut}(T_{\geq 0}, U_0, R_0)$ of tree $T_{\geq 0}(U_0, R_0)$ is:

$$\begin{aligned} T_{\geq j}(U_0, R_j) &= U_0^j T_{\geq 0}, & t_{\geq k}(U_k, R_0) &= R_0^k T_{\geq 0}, \\ T_j(U_{j,1}, R_j) &= U_0^j R_0^1 T_{\geq 0}, & t_k(U_k, R_{k,1}) &= R_0^k U_0^1 T_{\geq 0}, \end{aligned}$$

with identity non-moves $U_0^0, R_0^0, U_j^0, R_k^0$,

implied entities $t_{\geq 0} = T_{\geq 0}$, $t_0 = T_{\geq 1}$ and $T_0 = t_{\geq 1}$,

and the conjugated moves and conjugated arrows

$$\begin{aligned} R_j &= U^j R_0 U^{-j}, & U_k &= R^k U_0 R^{-k}, \\ U_{j,1} &= R^j U_0^1 R_0 U_0^{-1} R^{-j}, & R_{k,1} &= U^k R_0^1 U_0 R_0^{-1} U^{-k} \end{aligned}$$

Iterated functions and conjugated functions are themselves invertible (e.g. $U_0^i U_0^{-i} = U_j^0$), additive ($U_0^i U_0^j = U_0^{i+j}$), associative ($(U_0^i (U_0^j U_0^k)) = (U_0^i U_0^j) U_0^k = U_0^{i+j+k}$), and commutative ($U_0^i U_0^j = U_0^j U_0^i$). As is the case in any tree, the reversal of upward and rightward moves is *non-commutative* ($U_0^j R_0^k \neq R_0^k U_0^j$). The commutative diagram (Fig. 5) shows at a glance that reversal is enabled by the *conjugative* pair-of-pairs moves (proposition 1), as is true in any binary tree [9].

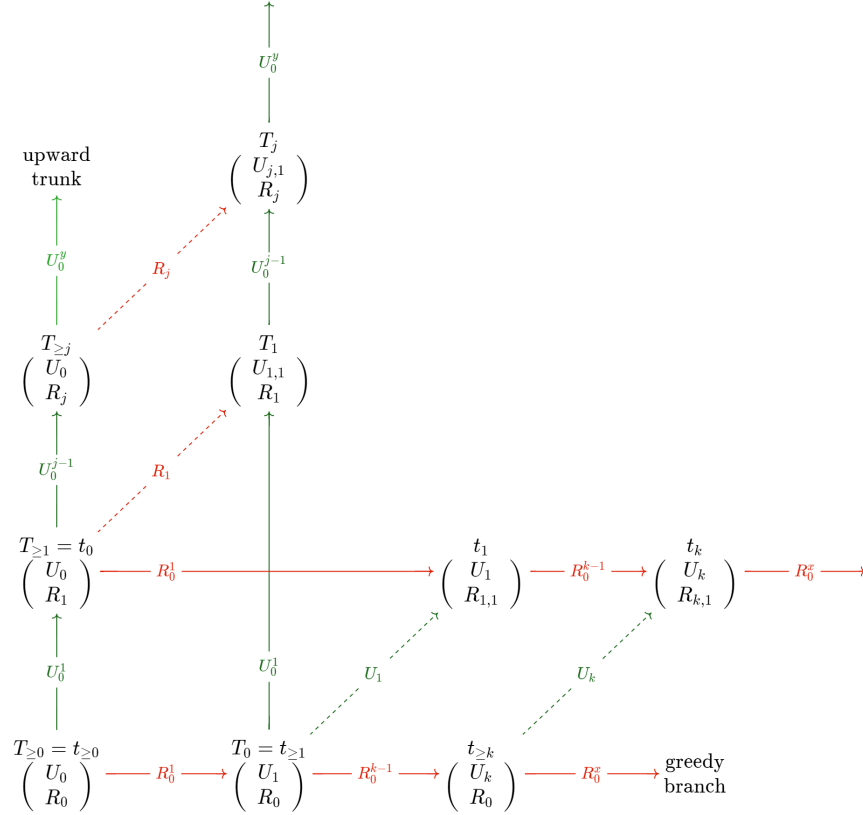


Figure 5: Commutative diagram of automorphism group $T_{\geq 0}(U_0, R_0)$

Legend: Arrows vs. brackets: outer vs. inner automorphism. Green vs. red arrows: Upward vs. rightward subtree tree generation. Superscript vs. subscript, solid vs. dashed arrows: iterations vs. conjugations. Iterations U_0^j, R_0^k : definitions 3 and 4. Conjugations $R_j, U_k, U_{j,1}, R_{k,1}$: definition 4.

Proposition 1

The two unary functions U_0 and R_0 generate the subtrees T_j , respectively t_k , the numbers of which are reachable through the moves $U_0^j R_0(T_{\geq 0})$ (Fig. 3), respectively $R_0^k U_0(T_{\geq 0})$ (Fig. 4), while obtaining a second conjugate root path $R_j U_0^j(T_{\geq 0})$, respectively $R_j U_0^j$, via the upward trunk, respectively the greedy branch (Suppl. Figs. S1). In short, $T_j = R_j U_0^j(T_{\geq 0}) = U_0^j R_0(T_{\geq 0})$ and $t_k = R_j U_0^j(T_{\geq 0}) = R_0^k U_0(T_{\geq 0})$.

Proof. Applying the definition of conjugacy, $f_i = g^i f_0 g^{-i}$, suffices.

$$T_j = R_j U_0^j(T_{\geq 0}) = U^j R_0 U_0^{-j} U_0^j(T_{\geq 0}) = U_0^j R_0(T_{\geq 0})$$

$$t_k = U_k R_0^k(T_{\geq 0}) = R_0^k U_0 R_0^{-k} R_0^k(T_{\geq 0}) = R_0^k U_0(T_{\geq 0}).$$

Tree T_j provides a root path of conjugated rightward arrows R_j inherited from tree $T_{\geq j}$ over $\Omega_j = \Omega_{\geq j} = U^j(\Omega_{\geq 0}) = U^j(4)$ on the trivial trunk. Tree t_k provides a root path of conjugated upward arrows U^k inherited from tree $t_{\geq k}$ over $\omega_j = \omega_{\geq j} = R^k(\Omega_{\geq 0}) = R^k(4)$ on the greedy branch.

4 Cumulative density of disjoint subtrees

The two unary functions U_0 and R_0 , both with natural numbers as arguments and outputs, generate $f_i = g^i f_0 g^{-i}$ -conjugates of U_0 and R_0 arrows in the subtrees T_1, T_2, T_3, \dots respectively t_1, t_2, t_3, \dots (Definition 4, Fig. 5). The Skolem–Noether automorphism theorem, named after Thoralf Skolem (1887–1963) and Emmy Noether (1882–1935), therefore implies the *existence* of a finite number of *congruence classes*—to be explained below—that generate all numbers in the node sets S_1, S_2, S_3, \dots and s_1, s_2, s_3, \dots of the correspondingly labeled subtrees [15, 16]. Despite the apparently chaotic nature of rightward iterations [1], a *constructive* proof of proposition 2 should, therefore, be possible.

Proposition 2. The functions U_0 and R_0 generate all congruence classes of the disjoint subtrees T_1, T_2, T_3, \dots and t_1, t_2, t_3, \dots (definition 4) in tree $T_{\geq 0}$, with a cumulative density that covers all branching numbers from set $S_{\geq 0}$ (Fig. 6).

Proposition 2 and its proof rely on linking congruence classes (15, 16) to the commutative diagram (Figs. 5–6). Thereby, Figure 6 summarizes that the functions U_0 and R_0 (Fig. 6, bottom left) generate congruence classes of disjoint subtrees of tree $T_{\geq 0}$, the density of which—denoted with ρ , Greek rho—includes all branching numbers (Fig. 6, top right).

4.1 Clock hands for subtree periodicity expansions

Congruence classes are familiar from divisions with remainders [17]. The odd numbers not divisible by 3, which are connected by $3n + 1$ to the branching nodes, comprise the arithmetic progressions $6i + 1$ and $6i + 5$, for $i = 0, 1, 2, \dots$. These progressions correspond to the congruence classes $[1, 5]_6$, with 6 as their minimum modulus, or *periodicity*—the alternative notation $1, 5 \equiv n \pmod{6}$ would accentuate congruence relations instead of congruence classes. Applying $3n + 1$ gives $3(6i + 1) + 1 = 18i + 4$ and $3(6i + 5) + 1 = 18i + 16$. This corresponds to the set $S_{\geq 0}$ of congruence classes $[4, 16]_{18}$ (Fig. 6, bottom left). The density of these classes amounts to 2 out of 18 successive numbers, giving $\rho = 2/18$ (denoted with Greek rho).

Periodicity expansions allow for partitions of the node set of a tree in the node sets of its subtrees. For example, the odd numbers $[1]_2$ can be partitioned after expanding their minimum periodicity to $[1, 3]_4$ or $[1, 3, 5, 7]_8$. The Collatz clock can be imagined as a clock with infinitely many hands that keep track of expanded, ever longer, periods in ever higher subtrees. Different periodicities must be aligned, as in planetary alignment and clock arithmetic.

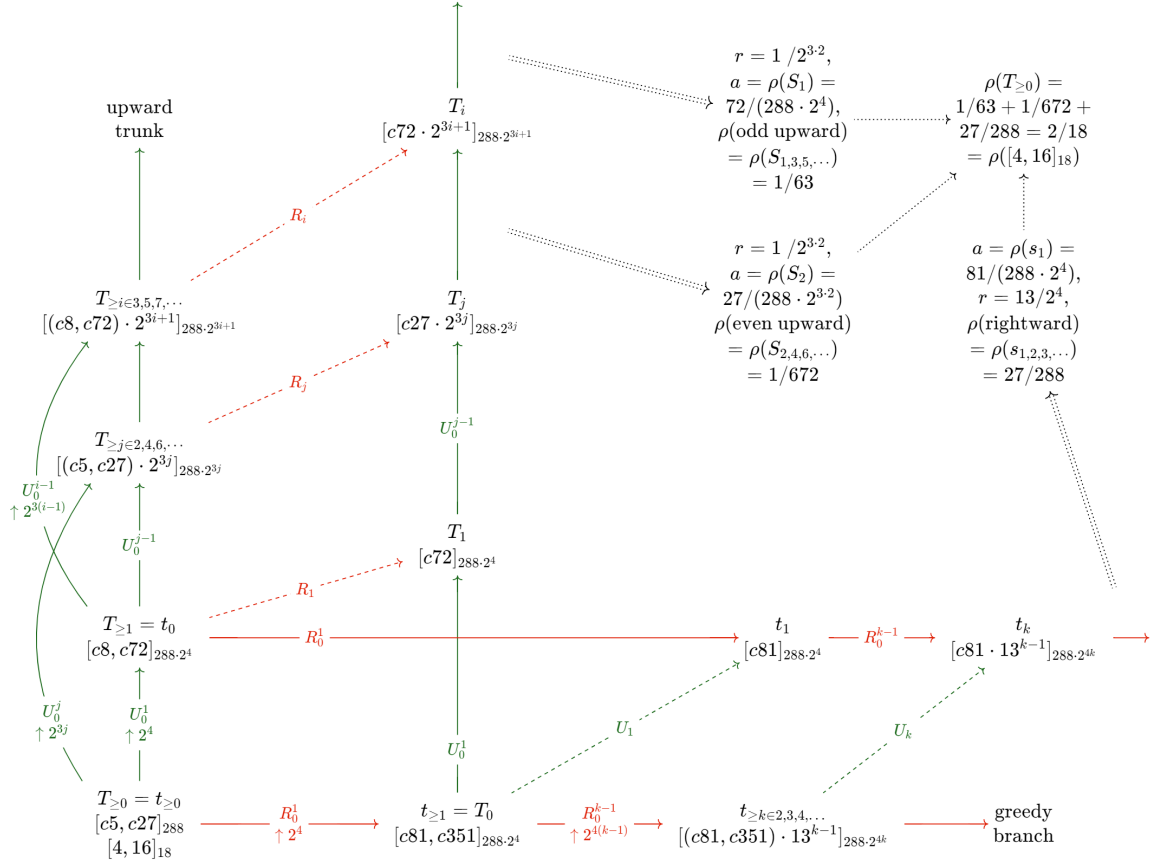


Figure 6. The Collatz clock

Legend. The sets of congruence classes $c5, c27, c8, c72, c81$ and $c351$ carry their count in their name (Suppl. S2, full listings). The subscripts denote their periodicity, or modulus. The conjugated functions U_1, U_k, R_1, R_i and R_j turn one of the two sets of congruence classes of a nested tree into the full node set of a disjoint tree.

The big hand of the clock turns every 60 minutes. The little hand turns every $12 \cdot 60 = 720$ minutes. Their *least common multiple period* $\text{lcm}(60, 720) = 720$ indicates that after 720 minutes for the first time a new period begins for both hands. The *alignment vector* $\vec{h} = [720/60, 720/720] = [12, 1]$ signifies that a least common multiple period consists of 12 periods for the big hand and 1 period for the little hand. The number of turns per least common period of the two hands is $12 + 1 = 13$, which gives their *density* $(12 + 1)/\text{lcm}(60, 270) = 13/720$. A *transformation matrix* tells which hands start running after a full turn of which hands. The slower turning additional hands—to keep track of ever-longer periods—give a *geometric series* with a steady density deceleration rate.

Thus, proposition 2 entails that, ultimately, the density of turns on the Collatz clock, which is the density of numbers delivered in disjoint subtrees by odd upward iterations, even upward iterations and rightward iterations, amounts to the density $\rho(S_{\geq 1}) = 2/18$ of branching numbers (Fig. 6, top right).

4.2 Upward function and rightward function

First, conditional specifications of the upward $U_0 : S_{\geq 0} \rightarrow S_{\geq 1}$ (def.5) and rightward $R_0 : S_{\geq 0} \rightarrow S_0$ functions are required, based on the two congruence classes $[4, 16]_{18}$ of branching numbers. These specifications include their least common multiple periodicity, their periodicity expansion, their alignment vector and the congruence classes in their upward co-domain $S_{\geq 1}$, respectively rightward co-domain S_0 .

Definition 5, upward function

$U_0 : S_{\geq 0} \rightarrow S_{\geq 1}; U_0(n) = \text{Argmin}_p(2^p n) \mid U_0(n) \in S_{\geq 0}$, specified as:

IF	THEN
$n =$	$\vec{p} \quad U_0(n) \quad \text{progression} \quad \text{lcm} \quad \vec{h}_U \quad S_{\geq 1} = [c5]_{288}$
$18i + 4:$	$2 \quad 4n \quad 72i + 16 \quad 288 \quad 4 \quad \{16, 88, 160, 232\}$
$18i + 16:$	$4 \quad 16n \quad 288i + 256 \quad 288 \quad 1 \quad \{256\}$

Upward traits: $U_0^2(n) = 64n$; upward periodicity expansions $\theta_{U1} = 288/18 = 16$ and $\theta_{U2} = 64$;

upward alignment vector $\vec{h}_U = [4, 1]$; density $\rho(S_{\geq 1}) = 5/288$.

$c5$ is a label for the 5 upward $S_{\geq 1}$ congruence classes.

Definition 6, rightward function

$R_0 : S_{\geq 0} \rightarrow S_0; R_0(n) = \text{Argmin}_p((n-1)/3) \cdot 2^p \mid R_0(n) \in S_{\geq 0}$ specified as:

IF	THEN
$n =$	$\vec{p} \quad R_0(n) \quad \text{progression} \quad \text{lcm} \quad \vec{h}_R \quad S_0 = [c27]_{288}$
$54i + 4:$	$2 \quad 4/3(n-1) \quad 72i + 4 \quad 288 \quad 4 \quad \{4, 76, 148, 220\}$
$54i + 16:$	$3 \quad 8/3(n-1) \quad 144i + 40 \quad 288 \quad 2 \quad \{40, 184\}$
$54i + 22:$	$4 \quad 16/3(n-1) \quad 288i + 112 \quad 288 \quad 1 \quad \{112\}$
$54i + 34:$	$1 \quad 2/3(n-1) \quad 36i + 22 \quad 288 \quad 8 \quad \{22, 58, 94, 130, 166, 202, 238, 274\}$
$54i + 40:$	$2 \quad 4/3(n-1) \quad 72i + 52 \quad 288 \quad 4 \quad \{52, 124, 196, 268\}$
$54i + 52:$	$1 \quad 2/3(n-1) \quad 36i + 34 \quad 288 \quad 8 \quad \{34, 70, 106, 142, 178, 214, 250, 286\}$

Rightward traits: rightward periodicity expansion $\theta_R = 288/54 = 2^4 3^{-1}$;

rightward alignment vector $\vec{h}_R(a) = [4, 2, 1, 8, 4, 8]$; density $\rho(S_0) = 27/288$.

$c27$ is a label for the 27 rightward S_0 congruence classes.

Let us discuss the upward function U_0 first. Given $n = 18i + 4$, the minimum argument $p = 2$ renders after substitution in $2^p n$ a branching number $4 \cdot 18i + 16$ belonging to $[4, 16]_{18}$. The lower value $p = 1$ gives non-branching numbers $2 \cdot 18i + 8$. Consequently, $U(n) = 4n$ (Fig. 2; *light green*), giving the arithmetic output progression $4(18i + 4) = 72i + 16$, which is the series $16, 88, 160, 232, \dots$ with 72 as its intrinsic periodicity. Given $n = 18i + 16$ the minimum argument is $p = 4$ (Definition 4; second row). Consequently, $U(n) = 16n$ (Fig. 2; *bright green*), giving the output progression $16(18i + 4) = 288i + 256$ with $288 = 4 \cdot 72$ as its periodicity. Lower values $p = 1$, $p = 2$, and $p = 3$ give numbers outside the branching congruence classes $[4, 16]_{18}$. Their least common multiple output periodicity becomes $v_{\geq 1} = \text{lcm}(72, 288) = 288$, with an implied upward alignment vector $\vec{h}_U = [4, 1]$. Five congruence classes $c5$ (Fig. 6), therefore, define the upward node set $S_{\geq 1} = [16, 88, 160, 232, 256]_{288} = [c5]_{288}$. Its density amounts to $\rho_{\geq 1} = 5/288$, and its

upward expansion after one iteration is $\theta_{U1} = 288/18 = 16$. Because the upward function U_0 turns input class 4 into output class 16, and vice versa (note that $256 = 16 \cdot 18 + 4$), the expansion after two iterations is $\theta_{U2} = 64$, with as the invariable outcome $U_0^2(n) = 64n$.

We derive the rightward function similarly. Compensation for the $(n-1)/3$ start of rightward paths requires an argument periodicity of $3 \cdot 18 = 54$ with six argument congruence classes, being $[4, 16, 22, 34, 40, 52]$. This result gives the minimum powers $\vec{p} = [2, 3, 4, 1, 2, 1]$, a least common multiple output periodicity of 288, a rightward alignment vector $\vec{h}_R = [4, 2, 1, 8, 4, 8]$, and a rightward periodicity expansion factor $\theta_R = 288/54 = 2^4 3^{-1}$. Compared to the upward function U_0 , the rightward function R_0 gives 27 other, *disjoint*, output congruence classes modulo 288, labeled as $c27$. The combined density of $\rho(S_{\geq 1}) = \rho([c5]_{288}) = 5/288$ and $\rho(S_0) = \rho([c27]_{288}) = 27/288$ amounts to the density $\rho_{\geq 0} = 2/18$ of branching nodes indeed—since $\rho([4, 16]_{18}) = 2/18$.

4.3 Density of disjoint upward subtrees

Separate density calculations for even and odd upward iterations are facilitated by the invariable upward expansion factor $\theta_{U2} = 64$, with $U_0^2(n) = 2^{3 \cdot 2} n$ after every second upward iteration.

Given the partition $S_{\geq 0} = \{S_{\geq 0}, S_0\} = [c5, c27]_{288}$ (defs. 5 and 6), the nested node set $S_{\geq j}$ of any even tree $T_{\geq j}$, for $j = 0, 2, 4, \dots$, can be partitioned in congruence classes $[(c5, c27) \cdot 2^{3j}]_{288 \cdot 2^{3j}}$. The conjugated function R_j makes the congruence classes $c27 \cdot 2^{3j}$ of the nested tree $T_{\geq j} = U_0^j(T_{\geq 0})$, $[(c5, c27) \cdot 2^{3j}]_{288 \cdot 2^{3j}}$, the full node set of the disjoint tree $T_j = R_j U_0^j(T_{\geq 0})$. This finding indicates a geometric series, with density $s = a/(1-r)$. Here, a is the density of the first even upward tree $\rho(T_{\geq 2}) = 27/(288 \cdot 2^6)$, whereas $r = 1/2^{3 \cdot 2}$ is the inverse of the upward expansion factor, and $s = \rho(S_{2,4,6,\dots}) = 1/672$ is the cumulative density of even upward iterations collected in the disjoint even upward trees $T_2, T_4, \dots, T_j, \dots$ (Fig. 6).

The upward expansion factor $\theta_{U1} = 16 = 2^4$ expands the five congruence classes $c5_{\geq 1}$ in the node set $S_{\geq 1}$ of tree $T_{\geq 1}$ to $5 \cdot 16 = 80$ congruence classes, namely $[16 + 0 \cdot 288, 88 + 0 \cdot 288, \dots, 232 + 15 \cdot 288, 256 + 15 \cdot 288]_{288 \cdot 2^4}$ (with \dots indicating 76 unspecified classes; full listings in Suppl S2). The partition of set $S_{\geq 1}$ in $\{S_{\geq 2}, S_1\} = [c8, c72]_{288 \cdot 2^4}$ is based both on the upward alignment vector $\vec{h}_U = [4, 1]$ and the $[15, 12]$ distribution of rightward congruence classes $c27$ between $[4]_{18}$ and $[16]_{18}$. Congruence class $[4]_{18}$ includes 15 rightward congruence classes, namely $[4, 22, 40, 58, 76, 94, 112, 130, 148, 166, 184, 202, 220, 238, 274]_{288}$. Of the upward congruence classes $c5$, only $[256]_{288}$ is included in $[4]_{18}$. Counting gives $4 \cdot 15 + 12 \cdot 1 = 72$ congruence classes in set $S_1 = [c72]_{288 \cdot 2^4}$ of the disjoint tree T_1 , labeled as $c72$, next to $4 \cdot 1 + 1 \cdot 4 = 8$ congruence classes in $S_{\geq 2} = [256, 1408, 2560, 3712, 1024, 2176, 3328, 4480]_{288 \cdot 2^4}$, labeled as $c8$. Given $U^2(n) = 2^{3 \cdot 2}(n)$, the bi-partitioned node set $S_{\geq i}$ of any nested odd upward tree $T_{\geq i}$ is, therefore, $[c8, c72]_{288 \cdot 2^{3(i-1)+4}} = [c8, c72]_{288 \cdot 2^{3i+1}}$. The basic operation $3i+1$ re-occurs in the odd upward periodicity as the power of 2. Hence, the node set S_i of any disjoint odd tree $T_i = R_i U_0^i(T_{\geq i})$ is $[c8, c72]_{288 \cdot 2^{3(i-1)+4}} = [c72]_{288 \cdot 2^{3i+1}}$. Applying $s = a/(1-r)$ to odd upward subtrees gives $a = \rho(T_1) = 72/4608$, again $r = 1/64$, and $s = \rho(S_{1,3,5,\dots}) = 1/63$ as the cumulative density of odd upward trees $T_1, T_3, \dots, T_i, \dots$ (Fig. 6).

4.4 Density of disjoint rightward subtrees

As in definition 6, the rightward paths starting with $(n-1)/3$ require a three times higher argument periodicity for each rightward iteration, giving a partition modulo $3 \cdot 288 = 864$ with $3 \cdot 5 = 15$

upward classes from $c5 \cdot 3$. The output of the first rightward iteration depends on their distribution over the rightward argument congruence classes $[4, 16, 22, 34, 40, 52]_{54}$, which is $[\{544\}, \{16, 232, 448, 664\}, \{832\}, \{88, 304, 520, 736\}, \{256\}, \{160, 376, 592, 808\}]$. Counting their successive numbers gives $[1, 4, 1, 4, 1, 4]$.

The transformation matrix T indicates how the rightward function $R(n)$ distributes its outputs over the rightward congruence classes $[4, 16, 22, 34, 40, 52]_{54}$ that become arguments in the next rightward iteration. The arguments $[4, 16, 22, 34, 40, 52]_{54}$ produce, after 3 periods of 54, periodically the triplets $[\{4, 22, 40\}, \{40, 22, 4\}, \{4, 22, 40\}, \{22, 4, 40\}, \{52, 16, 34\}, \{34, 16, 52\}]_{54}$ of congruence classes. For example, for $a = 40$, the arguments 40, 94, 148, 202, 256, 310, 364, 418, 172, ... give the rightward output progression 52, 124, 196, 268, 340, 412, 484, 556, 628, ..., in which each successive triplet reduces to the congruence classes triplet $[52, 16, 34]_{54}$. The 6 by 6 transformation matrix T , therefore, holds $[1, 0, 1, 0, 1, 0]$ as its first 4 rows and $[0, 1, 0, 1, 0, 1]$ as its last two rows. Post-multiplication by T gives triplets of argument congruence classes for the next rightward iteration, and, hence, a multiplication of the argument periodicity with 3, a rightward expansion factor of $3\theta_R = 16/3 = 2^4$, and periodic rightward orbits of any length (Suppl. S3). Scalar multiplication with the rightward alignment vector $\vec{h}_R = [4, 2, 1, 8, 4, 8]$ (definition 5) and matrix post-multiplication with T gives for the rightward tree t_1 the node set $s_1 = R_0(S_{\geq 1}) = (\vec{\#}_{\geq 1} \vec{h}_R) \cdot T = [15, 12, 15, 12, 15, 12]_{288 \cdot 2^4} = [c81]_{288 \cdot 2^4}$, with $c81$ denoting the congruence classes $[40, 58, 106, \dots, 12490, 12586, 12634]_{288 \cdot 2^4}$, with 75 congruence classes unlisted (Suppl. S2). The k 'th iteration gives $s_k = U_k R_0^k(S_{\geq 0}) = R_0^k(S_{\geq 1}) = (\vec{\#}(s_{k-1}) \vec{h}_R) \cdot T = [c81 \cdot 13^{k-1}]_{288 \cdot 2^{4k}}$ as the node set of any disjoint rightward tree t_k . The conjugated function U_j makes $c81$ the full node set of the disjoint tree $t_k = U_k R_0^k(T_{\geq 0})$. The same reasoning can be used to derive $[(c81, c341) \cdot 13^{k-1}]_{288 \cdot 2^{4k}}$ as the node set of the nested tree $t_{\geq k}$, with $c243 = [4, 22, 34, \dots, 12622, 12658, 12670]$.

Applying $s = a/(1 - r)$ gives $a = \rho(t_1) = 81/(288 \cdot 2^4)$, a density growth of $r = 13/16$, and $s = \rho(s_{1,2,3,\dots}) = 27/288$ as the cumulative density of the disjoint rightward trees $t_1, t_2, \dots, t_k, \dots$ (Fig. 6).

4.5 Density of the entire Collatz tree

The cumulative density of the disjoint node sets of the disjoint odd upward, even upward and rightward subtrees $T_1, T_2, T_4, \dots, T_2, T_4, T_6, \dots$ and t_1, t_2, t_3, \dots , holding all generations of successors in the binary Collatz tree $T_{\geq 0}$, amounts to $\rho(S_{1,2,3,\dots}, s_{1,2,3,\dots}) = 1/63 + 1/672 + 27/288 = 5/288 + 27/288 = 2/18$. This cumulative density proves proposition 2, because it is the density of all branching numbers. The greedy branch OEIS A225570 is rightly called *greedy* [4], because 27/32 of the branching numbers are on rightward trees rooted in the greedy branch rather than in the upward trunk. Together with the density of non-branching numbers, $\rho_{-1} = 16/18$, the density of numbers in the Collatz tree is 1, proving $\mathbb{N} = N_c$. The Collatz tree includes all natural numbers. Isolated trajectories do not exist.

5 Discussion

As anticipated by its proposer (4), our proof of the Collatz conjecture was substantially facilitated by connecting elementary number theory and elementary graph theory. Its proof was not “hopeless, absolutely hopeless”, as allegedly stated by Paul Erdős [1].

Recently, Terence Tao already delivered a logarithmic density proof of the Collatz conjecture for “almost all” numbers based on the *Syracuse* tree [3]. The Syracuse function connects any *odd* number n directly to the next *odd* number $\text{Syr}(n)$ obtained by iterations of the Collatz function. Its inverse $\text{Syr}^{-1}(n)$ thereby connects n to infinitely many successors with powers $p \in \mathbb{N}$, where both n and $\text{Syr}^{-1}(n) = (2^p n - 1)/3$ are odd. For example, $n = 1$ is connected by the p -values $2, 4, 6, 8, \dots$ in parallel to $1, 5, 21, 85, \dots$, the $3n+1$ map of which is the *serial* upward trunk $4 \rightarrow 16 \rightarrow 64 \rightarrow 256 \dots$ in the Collatz tree (Fig. 1).

Numbers in the binary Collatz tree $T_{\geq 0}$ with its cyclic root $\Omega_{\geq 0} = 4$ have two successors (Fig. 1). This propagation differs from the number line with one successor, and from prime factorization in which each prime is both the ancestor of infinitely many higher primes, for example $3 \rightarrow 5 \rightarrow 7 \rightarrow \dots$ and the ancestor of a cyclic power orbit, for example $3 \rightarrow 9 \rightarrow 27 \rightarrow \dots$ [17, 18]. Each Collatz tree number has a unique binary root path of *upward* or *rightward* steps (Fig. 2: $160 \rightarrow 1, 0, 1$). This is curiously reminiscent of prime factorization, which maps the natural numbers to unique sequences of powers of successive primes ($160 \rightarrow 2^5 \cdot 3^0 \cdot 5^1 \rightarrow 5, 0, 1$). The binary Collatz tree with two successors for each of its numbers may belong to a family of infinite number trees with finite numbers of successors.

The unary functions generating the automorphism group of the Collatz tree may resemble functions for modeling conjugate replication, regeneration, and reproduction in physics, biology, human learning or social networking. The Collatz clock may be helpful in other avenues already explored by Collatz sequences, such as pseudo-random number generation [19], encryption [20] and watermarking [21] — digital elements of our daily lives that are increasingly susceptible both to illegal denials of access and illegal violations of privacy.

Ancillary Materials. *ElaborationsCollatzTree.pdf* gives plots of the second path to generate subtrees (S1), full lists of the congruence classes in Figure 6 (S2) and additional plots on the periodicity of rightward orbits (S3). *Math12CollatzTree21.nb*, with additionally its static pdf, is the Mathematica 12 notebook underlying the paper.

Acknowledgements. The authors are grateful to the readers for their helpful, sometimes reluctant, comments on the earlier versions. In them, we based the density proof of the conjecture on the congruence classes $[1, 5]_6$ of numbers that are attached via $3n+1$ to the branching numbers $[4, 16]_{18}$. Its transfer to the branching numbers themselves, resulting in three times lower densities, makes the proof more transparent. Doubt that the subsets of numbers whose densities were calculated came entirely from ever higher pruned nested subtrees is now addressed by showing that these subsets are the full node sets of its disjoint subtrees—based on a new definition of the automorphism group of the binary tree with two unary functions rather than a binary splitting function. We especially thank Christian Koch and Eldar Sultanow, also for their Python / Github implementation [22]. We are greatly indebted to Klaas Sikkel for detailed comments in the run-up to the first arXiv version published on September 1st 2020, also on the notation of subtrees.

Works [22] [23] [24] from the references below are quoted in the ancillary materials.

References

- [1] J. C. Lagarias, *The Ultimate Challenge: The $3x + 1$ Problem*. Providence: AMS, 2010.
- [2] E. Roosendaal, “On the $3x+1$ problem,” <http://www.ericr.nl/wondrous/>, Last update before writing: December 10th 2021, 2020.
- [3] T. Tao, “Almost all orbits of the Collatz map attain almost bounded values,” *arXiv*, vol. 1909.03562, 2019.
- [4] OEIS Inc., “The online encyclopedia of integer sequences,” <https://oeis.org/A225570>, 1964-..
- [5] M. Chamberland, “A $3x+1$ survey: number theory and dynamical systems,” In: J.C. Lagarias, *The Ultimate Challenge*.
- [6] A. Kontorovich and J. C. Lagarias, “Stochastic models for the $(3x + 1)$ and $(5x + 1)$ problems and related problems,” In: J.C. Lagarias, *The Ultimate Challenge*.
- [7] A. Kontorovich, “The simplest math problem no one can solve - Collatz conjecture, interview with Veritasium,” <https://www.youtube.com/watch?v=094y1Z2wpJg>, 2021.
- [8] L. Collatz, “On the motivation and origin of the $(3n + 1)$ -problem,” In: J.C. Lagarias, *The Ultimate Challenge*.
- [9] A. M. Brunner and S. Sidki, “On the automorphism group of the one-rooted binary tree,” *Journal of Algebra*, vol. 195, no. 2, pp. 465–486, 1997.
- [10] F. Harary, *Graph theory*. Reading, MA: Addison-Wesley, 1965.
- [11] G. Valiente, *Algorithms on trees and graphs*. Berlin: Springer, 2021.
- [12] D. Hilbert, *Über das Unendliche*, pp. 730–731. Heidelberg: Springer, 1924.
- [13] M. Dehn, “Über unendliche diskontinuierliche Gruppen,” *Mathematische Annalen*, vol. 71, no. 1, pp. 116–144, 1911.
- [14] B. E. Nucinkis and S. S. John-Green, “Quasi-automorphisms of the infinite rooted 2-edge-coloured binary tree,” *Groups, Geometry, and Dynamics*, vol. 12, no. 2, pp. 529–570, 2018.
- [15] E. Noether, “Hyperkomplexe Grössen und Darstellungstheorieen,” *Mathematische Zeitschrift*, vol. 30, pp. 641–692, 1929.
- [16] E. Noether and W. Schmeidler, “Moduln in nichtkommutativen Bereichen,” *Mathematische Zeitschrift*, vol. 8, pp. 1–35, 1920.
- [17] M. H. Weissman, *An illustrated theory of numbers*. Providence: AMS, 2017.
- [18] B. Fine and G. Rosenberger, *Number Theory: An introduction via the distribution of primes*. Boston: Birkhäuser, 2007.
- [19] D. Xu and D. E. Tamir, “Pseudo-random number generators based on the Collatz conjecture,” *International Journal of Information Technology*, vol. 11, no. 3, pp. 453–459, 2019.
- [20] D. Renza, S. Mendoza, and D. M. Ballesteros L, “High-uncertainty audio signal encryption based on the Collatz conjecture,” *Journal of Information Security and Applications*, vol. 46, pp. 62–69, 2019.
- [21] H. Ma, C. Jia, S. Li, W. Zheng, and D. Wu, “Xmark: Dynamic software watermarking using Collatz conjecture,” *IEEE Transactions on Information Forensics and Security*, vol. 14, no. 11, pp. 2859–2874, 2019.
- [22] E. Sultanow, C. Koch, and S. Cox, “Collatz sequences in the light of graph theory,” <https://doi.org/10.25932/publishup-43008>, <https://github.com/c4ristian/collatz>, 2020.
- [23] D. R. Hofstadter, *Gödel, Escher, Bach: an eternal golden braid*, vol. 13. New York: Basic books, 1979.
- [24] S. Wolfram, *The Mathematica® book* (program version 12). Cambridge: Cambridge University Press, <https://www.wolfram.com/mathematica/>, 1989.